

# Measurement of Three-Dimensional Velocities of Spray Droplets Using the Holographic Velocimetry System

**Yeon-Jun Choo, Bo-Seon Kang**

Dep. of Mechanical Engineering, Chonnam Nat'l University 300,  
Young bong-Dong, Buk-Gu, Kwangju, 500-757, Korea

In this study, the holographic particle velocimetry system was used to measure the sizes and velocities of droplets produced by a full cone spray nozzle. As a preliminary experiment, the velocities of glass beads on a rotating disk were measured with uncertainty analysis. The error of the particle velocity measured by the holographic method was 0.75 m/s, which was 4.5 % of the known velocity. The spray droplet velocities ranged from 10.3 to 13.3 m/s with average uncertainty of  $\pm 1.6$  m/s, which was  $\pm 14$  % of the mean droplet velocity. The uncertainty of the optical axis component was very high due to the long depth of field of droplet images, which is inherent feature of holographic system using forward-scattering object wave of particles.

## 1. Introduction

The flow fields in many engineering areas have many complexities as well as being three dimensional in nature. In recent years, the focus of research on flow field measurement tools has concentrated on three dimensional velocity measurements. Even though the extension of 2-D PIV to 3-D seems to be a reasonable choice from a short-term standpoint, a holographic method might be an ultimate solution, because of its superiority in the realization of 3-D fields. However, many problems must be overcome because the holographic system remains at laboratory-development status level.

As for the spray diagnostic systems, considerable advances in laser instruments now make it possible to obtain reliable data upon droplet sizes and velocities in dilute sprays. However, they are inherently limited in denser spray regions. In addition, no information on the spray structure can be provided. On the other hand, the holographic technique re-produces the frozen spray, from which sizes and 3-D velocities of droplets and the spray structure can be investigated. The holographic technique has been widely used in research on particle sizing for some time [1]. Recently, interest in the use of holography as a tool for 3-D particle velocity determination has been increased. The holographic particle velocimetry systems reported can be classified into two categories; 1) Direct measurements of sizes and displacements from particle images [2-8] and 2) Holographic PIV, which extends the correlation technique used in 2-D PIV to three dimensions [9-12].

This paper reports the results of a preliminary study at the intermediate stage of the development of the holographic velocimetry system for spray droplets. Validation experiments were conducted to compare the holographic measurement results of the sizes and velocities of glass beads on a rotating disk with known values. Uncertainty analysis was performed to identify the sources of relevant errors. Finally, the sizes and 3-D velocities of spray droplets were measured by the manual image processing.

## 2. Experimental apparatus and methodology

Figure 1 shows a schematic of the holographic recording system. The light source was a twin Nd-YAG laser (Brilliant B, Quantel), which generated wavelength of 532 nm and 300 mJ output energy laser beams. The pulse interval was controllable from 1 to 900  $\mu$ s. The short pulse duration (10 ns) used assured the freezing of all moving particles.

The light was separated using a beamsplitter, which divided the beam into reference and object beams. The object beam was expanded and collimated to a diameter of 10 cm using a beam expander. This plane wave was passed through the test section and finally was intercepted at the holographic glass plate. A diffuser was positioned before the test section to provide a uniform background and to decrease the depth of field of the particle image.

The velocity measurement results obtained by holographic method should be verified against some kind of experimental system, in which the particle velocities are already known and easily changed. For this purpose, we used small glass beads on a rotating disk. The system consists of a driving motor and a horizontally positioned rotating disk of diameter 300 mm on which glass beads were attached to the tips of thin wires. Similar size of glass beads was located at each radius of 85, 105, 115, and 125 mm. The rotating speed was controllable to 3,000 rpm. The possible maximum velocity of glass beads located at periphery of the disk was 40 m/s.

After validation experiments, the sizes and velocities of real spray droplets were measured. A high-pressure  $N_2$  gas cylinder is used to pressurize a liquid reservoir to direct non-fluctuating stable liquid to flow to a commercial full cone spray nozzle. Water is injected with injection pressure of 245 kPa through the 1.0 mm nozzle hole.

The recorded holograms were reconstructed and analyzed using an image processing system as shown in Fig. 2. The laser was a diode-pumped crystal laser of the same wavelength for recording. Real particle images were captured. The digital CCD camera (Kodak Co., 1,024  $\times$  1,024 pixels) was moved automatically using a three axes translation stage (PI) and positioned with a resolution of 30  $\mu$ m. The measurements of sizes and moving distances of particles were performed manually using image processing software (Inspector, Matrox Inc.).

## 3. Experimental results and discussion

### 3.1. Validation experiments

To verify the velocity measurements made using the holographic method, double pulse images of glass beads located at a radius of 125 mm at a rotation speed of 813 or 1,284 rpm were analyzed. Fig. 3 shows the reconstructed double pulse image of particles. The left and right particles in each figure

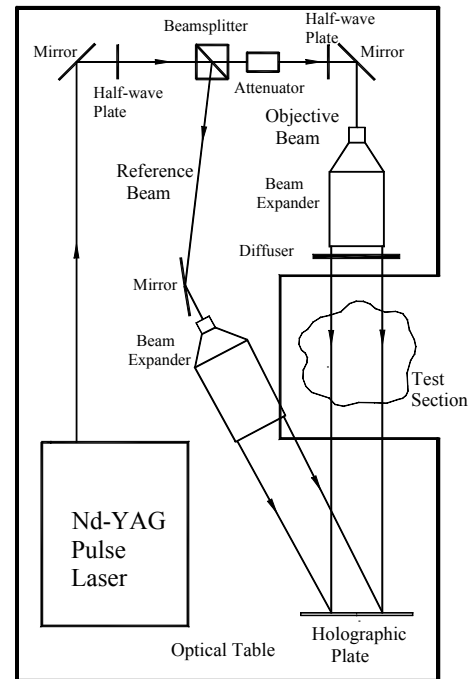


Fig. 1 Schematic diagram of the holographic recording system

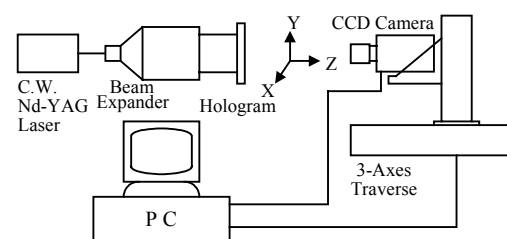


Fig. 2 Image reconstruction and processing system.

were recorded at the first and second pulses and Fig. 3 (a) focused on the left particle and Fig. 3 (b) on the right particle.

The actual velocity of a particle is

$$V_a = R \times \omega \quad (1)$$

So, the uncertainty,  $u_{V,a}$ , can be expressed as follows by the propagation of uncertainty [13].

$$u_{V,a} = \sqrt{\left(\frac{\partial V_a}{\partial R} u_R\right)^2 + \left(\frac{\partial V_a}{\partial \omega} u_\omega\right)^2} = \sqrt{(\omega u_R)^2 + (R u_\omega)^2} \quad (2)$$

Here,  $u_R$  is the uncertainty in the radius measurement by Vernier caliper and this is  $\pm 0.025$  mm. The uncertainty of the rotation speed of the disk,  $u_\omega$ , consists of the zero-order uncertainty of the instrument ( $\pm 0.5$  rpm) and the precision error.

Particle velocities by the holographic technique are obtained by dividing the distance moved by the particles by the pulse interval. The conversion factor,  $F$ , was obtained by using the hologram of a 5 mm scale. The distances moved by particles in the  $x$  and  $y$  directions were obtained by multiplying the number of pixels between the centers of particles at each pulse by the conversion factor. Therefore, the uncertainty of distance measurement in the  $x$  and  $y$  directions can be expressed as

$$u_{D_i} = \sqrt{\left(\frac{\partial D_i}{\partial F} u_F\right)^2 + \left(\frac{\partial D_i}{\partial N} u_N\right)^2} = \sqrt{(N u_F)^2 + (F u_N)^2} \quad (3)$$

One of inherent characteristics of particle holography using forward scattered light by particles is the very long depth of field of particle images in the optical axis. This characteristic causes considerable difficulty in the determination of particle positions in the optical axis. In the present study, several seemingly in-focus particle images were captured first by moving a CCD camera along the optical axis, and then the depth was determined by using the change in the gradient of gray values of particles and background or by the operator. The particle position in the  $z$  direction was determined as the center of this depth. As for the uncertainty of distance measurement in the  $z$  direction,  $u_{D_z}$ , the depths for one particle for the cases of 813 and 1,284 rpm, were  $\pm 0.06$  and  $0.07$  mm, respectively. So,  $u_{D_z}$  was assumed to be twice these values, namely,  $u_{D_z} = \pm 0.12$  and  $0.14$  mm.

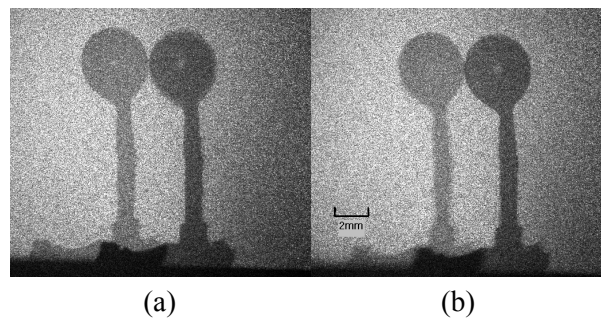


Fig. 3 Holographically reconstructed double image of particle; particle image of (a) first pulse (b) second pulse is focused.

**Table 1** Comparison of actual glass bead velocities with measured values.

Actual Velocity (m/s)		Measured Velocity (m/s)			Error (m/s)
RPM	Va	Vx	Vz	Vm	
813 ± 2.05	10.637 ± 0.027	5.850 ± 0.165	8.550 ± 0.224	10.365 ± 0.207	0.272 (2.6%)
1284 ± 1.37	16.799 ± 0.020	8.316 ± 0.280	13.722 ± 0.285	16.045 ± 0.284	0.754 (4.5%)

The components of particle velocity in each direction are calculated by division of moved distances by the pulse interval so the uncertainty of particle velocity in each direction is expressed as

$$u_{Vi} = \sqrt{\left(\frac{\partial V_i}{\partial D_i} u_{D_i}\right)^2 + \left(\frac{\partial V_i}{\partial \Delta t} u_{\Delta t}\right)^2} = \sqrt{\left(\frac{1}{\Delta t} u_{D_i}\right)^2 + \left(\frac{D_i}{\Delta t^2} u_{\Delta t}\right)^2} \quad (4)$$

The uncertainty of the particle velocity measured by the holographic method,  $u_{V,m}$ , is calculated from

$$u_{V,m} = \sqrt{\left(\frac{\partial V}{\partial V_x} u_{V_x}\right)^2 + \left(\frac{\partial V}{\partial V_y} u_{V_y}\right)^2 + \left(\frac{\partial V}{\partial V_z} u_{V_z}\right)^2} \quad (5)$$

Based on above analysis, the actual and measured velocities of the glass beads with their uncertainties and the relative errors of measurements are summarized in Table 1. The greatest error of the particle velocity measured by the holographic technique is 0.75 m/s, which is 4.5 % of the actual velocity.

### 3.2. Droplet size and velocity measurements

The velocities of spray droplets and uncertainties in the measurements are obtained using the same method described before except for uncertainty in the z direction. The uncertainty in the determination of particle positions in the z direction is related to the depth of field of the particle. According to the Meng's analysis [10] for particles recorded and reconstructed using the holographic system, the depth of field,  $\delta$ , depends on the size of the particles and the optical system used.

$$\delta = \beta \frac{d}{\Omega} \quad (6)$$

Here,  $\beta$  is a coefficient introduced to incorporate system-dependent sensitivity and  $\Omega$  is the effective aperture forming the holographic image.

Based on above analysis, the particle diameter was selected as a parameter for the uncertainty in the determination of a particle's position in

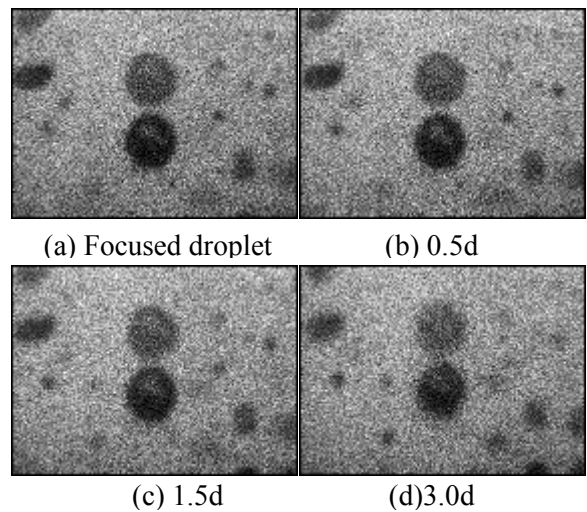


Fig. 4 Differences in focused droplet image due to the focal plane movement.

the  $z$  direction. To determine what fraction of diameter can be considered as the uncertainty, the focal plane of a camera was gradually moved from the focused position of droplet. Figure 4 shows the difference in droplet images due to the movement of the focal plane. Defocusing gradually becomes severe as the focal plane is moved over  $0.5d$  from the focused plane. Therefore,  $0.5d$  was selected as the uncertainty in the determination of a particle's position in the  $z$  direction, namely,  $u_{D_z} = \pm d$  mm. Supplementary experiments are underway to more accurately evaluate the magnitude of the uncertainty in the determination of a particle's position along the optical axis.

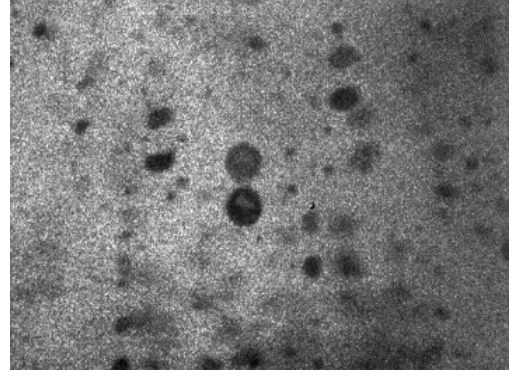


Fig. 5 Holographically reconstructed double pulse image of spray droplets.

Figure 5 shows a typical double pulse image of spray droplets. The measured results are summarized in Table 2. Each component and magnitude of droplet velocity is shown in Fig. 6 and 7, respectively.

The highest component of droplet velocity occurs in the  $y$  direction, namely, in the axis of the spray. These velocities range from 9.0 to 11.7 m/s. The average of the corresponding

**Table 2** Results of droplet velocity and diameter measurements.

No.	Position (mm)			Velocity (m/s)			V(m/s)	Diameter ( $\mu\text{m}$ )
	x	y	z	V <sub>x</sub>	V <sub>y</sub>	V <sub>z</sub>		
1	-1.35	5.92	15.73	-2.90 $\pm$ 0.39	10.93 $\pm$ 0.71	6.99 $\pm$ 4.76	13.29 $\pm$ 2.57	476 $\pm$ 24
2	-4.25	10.33	-2.00	-3.02 $\pm$ 0.54	10.71 $\pm$ 0.67	-2.33 $\pm$ 2.99	11.37 $\pm$ 0.89	299 $\pm$ 15
3	-11.52	16.48	-0.73	-4.42 $\pm$ 0.43	9.17 $\pm$ 0.58	-1.99 $\pm$ 1.33	10.37 $\pm$ 0.60	133 $\pm$ 7
4	-6.92	20.22	5.00	-5.14 $\pm$ 0.46	9.87 $\pm$ 0.62	3.33 $\pm$ 3.38	11.62 $\pm$ 1.13	338 $\pm$ 17
5	-4.12	27.74	-16.67	-0.79 $\pm$ 0.31	10.15 $\pm$ 0.64	-2.33 $\pm$ 3.30	10.45 $\pm$ 0.97	331 $\pm$ 17
6	8.83	38.33	26.33	1.39 $\pm$ 0.35	10.46 $\pm$ 0.67	4.67 $\pm$ 4.56	11.55 $\pm$ 1.94	457 $\pm$ 24
7	-10.14	45.59	-11.89	-1.55 $\pm$ 0.30	9.38 $\pm$ 0.60	-5.53 $\pm$ 3.53	10.99 $\pm$ 1.85	353 $\pm$ 18
8	-18.13	48.82	-17.33	-1.87 $\pm$ 0.32	9.17 $\pm$ 0.58	-6.67 $\pm$ 4.36	11.98 $\pm$ 2.48	437 $\pm$ 22
9	4.32	54.02	-27.67	1.55 $\pm$ 0.37	9.86 $\pm$ 0.62	-6.67 $\pm$ 2.53	12.01 $\pm$ 1.49	253 $\pm$ 13
10	17.32	58.12	11.40	3.89 $\pm$ 0.56	10.65 $\pm$ 0.71	0.82 $\pm$ 4.26	11.33 $\pm$ 0.75	426 $\pm$ 22
11	-4.75	60.22	26.70	-0.50 $\pm$ 0.41	9.97 $\pm$ 0.63	4.00 $\pm$ 5.06	12.49 $\pm$ 1.76	506 $\pm$ 26
12	-13.25	67.12	21.40	-1.95 $\pm$ 0.34	9.97 $\pm$ 0.63	3.33 $\pm$ 3.73	10.69 $\pm$ 1.30	373 $\pm$ 19
13	-12.51	73.21	25.60	-1.47 $\pm$ 0.28	10.66 $\pm$ 0.62	4.67 $\pm$ 3.33	11.73 $\pm$ 1.44	333 $\pm$ 17
14	1.09	74.21	26.00	0.53 $\pm$ 0.37	9.03 $\pm$ 0.65	8.80 $\pm$ 3.99	12.62 $\pm$ 2.83	399 $\pm$ 20
15	15.21	74.93	4.00	1.85 $\pm$ 0.35	10.05 $\pm$ 0.58	1.22 $\pm$ 2.95	10.29 $\pm$ 0.67	295 $\pm$ 15
16	9.15	75.56	-5.00	0.88 $\pm$ 0.38	10.29 $\pm$ 0.55	-6.67 $\pm$ 5.80	12.29 $\pm$ 3.28	581 $\pm$ 30
17	14.50	78.52	14.53	1.79 $\pm$ 0.29	11.68 $\pm$ 0.67	3.99 $\pm$ 4.38	12.48 $\pm$ 1.54	439 $\pm$ 23

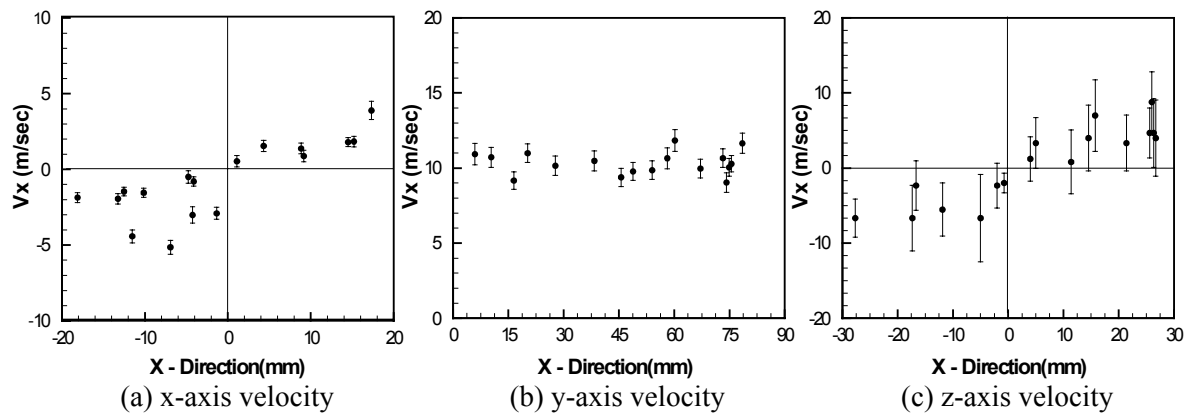


Fig. 6 Velocity components of droplets; (a) x-axis velocity (b) y-axis velocity (c) z-axis.

uncertainties is  $\pm 0.64$  m/s. The velocity component in the  $x$  direction varies from 0.5 to 5.1 m/s. The average uncertainty is  $\pm 0.4$  m/s. On the other hand, the velocity component in the  $z$  direction changes from 0.8 to 8.8 m/s and the average uncertainty is  $\pm 3.4$  m/s, which is very high compared with the relatively small uncertainties of the velocity components in directions normal to the optical axis. As explained before, this is due to the long depth of field of the droplet images in the optical axis, which is an inherent feature of the droplet images in the optical axis, which is an inherent feature of the holographic system using forward-scattering object wave of particles. The magnitude of the droplet velocities ranges from 10.3 to 13.3 m/s and the average uncertainty is  $\pm 1.6$  m/s. The relatively large uncertainties result from the large uncertainties in the optical axis and supplementary experiments are underway to improve the uncertainty in the optical axis.

The sizes of droplets are obtained by evaluating the equivalent diameter of droplets from the total area of droplet images. The sizes range from 133 to 581  $\mu\text{m}$ . The average uncertainty of size measurements is  $\pm 20$   $\mu\text{m}$ .

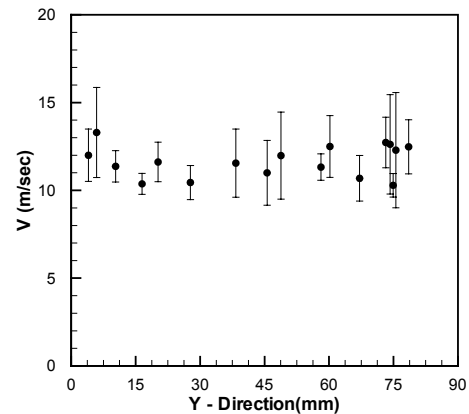


Fig. 7 Magnitude of droplet velocities.

#### 4. Conclusion

In this study, the sizes and velocities of droplets produced by a full cone spray nozzle were measured using the holographic velocimetry system with manual image processing. As a validation experiment, the velocities of glass beads on a rotating disk were measured and the results were compared with the known velocities obtained from the rotating speed of the disk. Uncertainty analysis was performed to identify the sources of all relevant errors and to evaluate their magnitudes.

The measurement results of velocities obtained using the holographic method compared reasonably well with the known values, within acceptable error ranges. To be specific, the error of the glass bead velocity measured by the holographic method was 0.75 m/s, which was 4.5 % of the known velocity. The spray droplet velocities ranged from 10.3 to 13.3 m/s with an average uncertainty of  $\pm 1.6$  m/s. Compared with the relatively small uncertainty in velocity components in the directions normal to the optical axis, that of the optical axis component is  $\pm 3.6$  m/s. This large uncertainty is attributed to the long depth of field of droplet images in the optical axis, which is an inherent feature of a holographic system using forward-scattering object wave of particles.

#### Acknowledgements

This work was supported by a grant No. R05-2000-000-00297-0 from Korea Science and Engineering Foundation.

#### Reference

- [1] Vikram C S 1979 *Particle Field Holography* (Cambridge University Press)
- [2] Feldmann O 1999 "Short-Time Holography and Holographic PIV Applied to Engineering Problems," *Applied Optical Measurements*, Springer-Verlag.

- [3] Haussmann G and Lauterborn W 1980 *Applied optics* 19 3529-35
- [4] Kang B S 1995 *A Holographic Study of The Dense Region of a Spray Created by Two Impinging Jets* Ph.D. Thesis Univ. of Illinois at Chicago
- [5] Lauterborn W and Hentschel W 1986 *Ultrasonics* 24 59-65
- [6] Prikryl I and Vest C M 1982 *Applied optics* 21 2541-7
- [7] Staselko D I and Kosnikovskii V A 1973 *Optics and Spectroscopy* 34 206-10.
- [8] Witherow W K 1979 *Optical Engineering* 18 249-55
- [9] Barnhart D H and Adrian R J 1994 *Applied Optics* 33 7159-70
- [10] Meng H and Hussain F 1995 *Applied Optics* 34 1827-40
- [11] Zhang J, Tao B and Katz J 1997 *Experiments in Fluids* 23 373-81
- [12] Zimin V, Meng H and Hussain F 1993 *Optical Letters* 18 1101-03.
- [13] Figliola R S and Beasley D E 1998 *Theory and Design for Mechanical Measurement* (John Wiley & Sons) 181-232
- [14] Oh D J, Choo Y J and Kang B S 2002 *Transactions of the KSME* 26 539-46